DALTON COMMUNICATION

Entrapment of a Pt–H bond by a cavity-shaped receptor

Catherine Wieser,[a] Dominique Matt,*[a] Loic Toupet,[b] Hervé Bourgeois[c] and Jean-Pierre Kintzinger[c]

[a] *Groupe de Chimie Inorganique Moléculaire, ECPM, Université Louis Pasteur, URA 405 CNRS, 1 rue Blaise Pascal, F-67008 Strasbourg Cedex, France*

[b] *Groupe Matière Condensée et Matériaux, Université de Rennes 1, Bât. 11B, Campus Beaulieu, F-35042 Rennes Cedex, France*

[c] *Laboratoire de Résonance Magnétique Nucléaire et Modélisation Moléculaire, UMR 50 CNRS/Bruker, Université Louis Pasteur, 1 rue Blaise Pascal, F-67070 Strasbourg Cedex, France*

A new platinum hydride was quantitatively formed in the reaction of *trans*-[PtH(Cl)(PPh_3)$_2$] with 5,11,17,23-tetra-*tert*-butyl-25,27-bis(diethylcarbamoylmethoxy)-26,28-bis(diphenylphosphinomethoxy)calix[4]arene; X-ray analysis and NMR studies showed that the hydrido ligand is directed into the hemispherical cavity induced around the platinum centre.

Calix[4]arenes are versatile platforms from which functional groups can be oriented so as to provide well defined cavities or clefts.[1] Exploitation of this property has led to the design and synthesis of numerous novel architectures displaying highly selective binding properties towards certain metal ions and/or facilitating specific detection of anionic species. Despite obvious attractions, little attention has been given to the isolation of calix[4]arene ligands bearing organometallic fragments as pendant arms,[2] and in particular we are unaware of any examples of transition-metal alkyls or hydrides encapsulated *inside* the molecular cavity. Specifically, calix[4]arenes having reactive organometallic species incorporated directly into the cavity in such a manner as to offer a partially-exposed catalytic site to incoming suitably-shaped substrates might be envisaged to display novel and attractive properties. As an approach to this ideal, we now report a unique calixarene-based complex in which a platinum-bound hydride ligand is *trapped* within the cavity defined by the four tethered arms.

Reaction of *trans*-[PtH(Cl)(PPh_3)$_2$] **1**[3] with diphosphine **2**[4] in CH_2Cl_2 resulted in quantitative formation of complex **3** (Scheme 1).† The monomeric nature of complex **3** was confirmed by vapour-phase osmometry, while its cone conformation was established by ^{13}C NMR.[5] The *trans* stereochemistry around the platinum atom was assigned on the basis of ^{31}P and ^1H NMR: J(P–Pt) 3122 and ^2J(P–$H_{hydride}$) 15 Hz.[6] The hydride ligand in **3** appears at δ −15.04 in the ^1H NMR ($CDCl_3$) spectrum (*cf.* δ −15.21 for **1**). Two-dimensional rotating-frame Overhauser enhancement spectroscopy (500 MHz) indicates unequivocally that the hydride ligand resides in

† Selected data for **3**. M.p. 254–255 °C. IR(KBr): 1658s ($\nu_{C=O}$) cm^{-1}. ^1H NMR ($CDCl_3$, 200 MHz): δ 7.93–7.91 and 7.42 (m br, 20 H, PPh_2), 7.12 (s, 4 H, *m*-ArH), 6.53 (s, 4 H, *m*-ArH), 5.35 [s with Pt satellites, 4 H, OCH_2PPh_2, J(HPt) = 33], 4.63 and 3.04 (AB spin system, 8 H, $ArCH_2Ar$, ^2J = 13.0), 4.12 (s, 4 H, OCH_2CONEt_2), 3.21 (q, 4 H, NCH_2CH_3, ^3J = 7.1), 2.77 (q, 4 H, NCH_2CH_3, ^3J = 7.1), 1.35 (s, 18 H, Bu^t), 1.01 (t, 6 H, NCH_2CH_3, ^3J = 7.0), 0.99 (t, 6 H, NCH_2CH_3, ^3J = 7.1), 0.81 (s, 18 H, Bu^t) and −15.04 [t with Pt satellites, 1 H, PtH, ^2J(HP) = 15, J(HPt) = 1150 Hz]. ^1H NMR (C_6D_6): δ −14.22 [t with Pt satellites, PtH, ^2J(HP) = 15, J(PtH) = 1150 Hz]. ^{13}C-{^1H} NMR ($CDCl_3$): δ 168.00 (s, C=O), 154.71–124.73 (aromatic C), 71.27 (s, OCH_2CONEt_2), 70.24 [t, OCH_2PPh_2, $|J(PC) + {}^3J(P'C)|$ = 51 Hz], 40.33 and 39.64 (2s, NCH_2CH_3), 33.96 and 33.51 [2 s, $C(CH_3)_3$], 31.93 (s, $ArCH_2Ar$), 31.67 and 31.07 [2 s, $C(CH_3)_3$], 14.18 and 12.99 (2s, NCH_2CH_3). ^{31}P-{^1H} NMR ($CDCl_3$, 36.43 MHz): δ 22.7 [s with Pt satellites, PPh_2, J(PPt) = 3122 Hz] [Found: C, 62.8; H, 6.75; N, 1.60. Calc. for $C_{82}H_{101}ClN_2O_6P_2Pt{\cdot}CH_2Cl_2$ (M_r = 1503.22 + 84.93): C, 62.75; H, 6.55; N, 1.75%]. Positive ion FAB MS, *m*/*z* (%): 1467 (100) [$M - Cl$]$^+$. Osmometry (CH_2Cl_2): M_{found} 1490.

For **4**. M.p. 188–190 °C. IR(KBr): 1653s ($\nu_{C=O}$) and 1057s (BF_4) cm^{-1}. ^1H NMR ($CDCl_3$): δ 7.49–7.08 (35 H, PPh_3 and PPh_2), 6.93 (s, 4 H, *m*-ArH), 6.27 (s, 4 H, *m*-ArH), 5.85 [s with Pt satellites, 4 H, OCH_2PPh_2, ^3J(HPt) = 52], 4.05 (s, 4 H, OCH_2CONEt_2), 3.88 and 2.68 (AB spin system, 8 H, $ArCH_2Ar$, ^2J = 13.0), 3.66 (q, 4 H, NCH_2CH_3, ^3J = 7.0), 3.02 (q, 4 H, NCH_2CH_3, ^3J = 7.0), 1.40 (t, 6 H, NCH_2CH_3, ^3J = 7.0), 1.28 (s, 18 H, Bu^t), 1.05 (t, 6 H, NCH_2CH_3, ^3J = 7.0), 0.74 (s, 18 H, Bu^t) and −4.31 [dt with Pt satellites, 1 H, PtH, $^2J(HP_{cis})$ = 16, $^2J(HP_{trans})$ = 168, J(HPt) = 774 Hz]. ^{13}C-{^1H} NMR ($CDCl_3$): δ 167.44 (s, C=O), 155.39–124.44 (aromatics), 73.21 [t, OCH_2PPh_2, $|J(PC) + {}^3J(P'C)|$ = 52 Hz], 72.18 (s, OCH_2CONEt_2), 40.83 and 40.25 (2s, NCH_2CH_3), 33.78 and 33.45 [2 s, $C(CH_3)_3$], 31.43 and 30.87 [2s, $C(CH_3)_3$], 30.07 (s, $ArCH_2Ar$), 14.08 and 13.16 (2s, NCH_2CH_3). ^{31}P-{^1H} NMR ($CDCl_3$): δ 22.3 [t with Pt satellites, PPh_3, ^2J(PP') = 20 Hz, J(PPt) = 2040], 14.38 [d with Pt satellites, PPh_2, ^2J(PP') = 20, J(PPt) = 2879 Hz] [Found: C, 64.80; H, 6.40; N, 1.45. Calc. for $C_{100}H_{116}BF_4N_2O_6P_3Pt{\cdot}0.5CH_2Cl_2$ (M_r = 1816.86 + 42.46): C, 64.90; H, 6.35; N, 1.50%]. Positive ion FAB MS, *m*/*z* (%): 1467.6 (100) [$M - PPh_3 - BF_4$]$^+$.

For **5**. M.p. 218–219 °C. IR(KBr): 1655s ($\nu_{C=O}$), 1606s ($\nu_{C=O}$) and 1060s (BF_4) cm^{-1}. ^1H NMR ($CDCl_3$): δ 7.84–7.40 (20 H, PPh_2), 7.18 and 7.05 (AB spin system, 4 H, *m*-ArH, ^4J = 3), 6.54 and 6.33 (2s, 4 H, *m*-ArH), 6.23 and 5.01 [ABXX' spin system with X,X' = P, 4 H, OCH_2PPh_2, ^2J(AB) = 12, $|J(AX) + J(AX')|$ = 10, J(BX) not determined], 4.32 and 3.59 (2s, 4 H, OCH_2CONEt_2), 4.32 and 3.31 (AB spin system, 4 H, $ArCH_2Ar$, ^2J = 13), 3.55 and 2.42 (AB system, 4 H, $ArCH_2Ar$, ^2J = 13), 3.77 (q, 2 H, NCH_2CH_3, ^3J = 7), 3.39 (q, 2 H, NCH_2CH_3, ^3J = 7), 3.11 (q, 2 H, NCH_2CH_3, ^3J = 7), 3.09 (q, 2 H, NCH_2CH_3, ^3J = 7), 1.41 (t, NCH_2CH_3, ^3J = 7), 1.36 (s, 18 H, Bu^t), 1.15, 1.08 and 0.94 (3t, NCH_2CH_3, ^3J = 7), 0.84 (s, 9 H, Bu^t), 0.75 (s, 9 H, Bu^t) and −22.95 [t with Pt satellites, 1 H, PtH, J(HPt) = 1306, ^2J(HP) = 15 Hz]. ^{13}C-{^1H} NMR ($CDCl_3$): δ 170.27 and 166.07 (2s, C=O), 155.49–125.21 (aromatics), 75.67 [t, OCH_2PPh_2, $|J(PC) + J(P'C)|$ = 48 Hz], 72.73 and 70.34 (2s, OCH_2CONEt_2), 40.87, 40.57 and 40.13 (NCH_2CH_3), 34.21, 33.73 and 33.59 [3s, $C(CH_3)_3$], 31.72, 31.09 and 30.98 [3s, $C(CH_3)_3$], 31.53 and 29.97 (2s, $ArCH_2Ar$), 14.33, 13.41, 13.19 and 13.05 (4s, NCH_2CH_3). ^{31}P-{^1H} NMR ($CDCl_3$): δ 24.8 [s with Pt satellites, PPh_2, J(PPt) = 3166 Hz] [Found: C, 61.40; H, 6.35; N, 1.75. Calc. for $C_{82}H_{101}BF_4N_2O_6P_2Pt{\cdot}0.75CH_2Cl_2$ (M_r = 1467.76 + 63.70): C, 61.40; H, 6.40; N, 1.75%]. Positive ion FAB MS, *m*/*z* (%): 1467 (100) [M^+].

For **6**. M.p. 252 °C (decomp.). IR (KBr): 1667s ($\nu_{C=O}$) and 2224m ($\nu_{C\equiv N}$) cm^{-1}. ^1H NMR ($CDCl_3$): δ 7.94–7.90 and 7.51–7.50 (20 H, PPh_2), 6.99 (s, 4 H, *m*-ArH), 6.52 (s, 4 H, *m*-ArH), 6.09 [s with Pt satellites, 4 H, OCH_2PPh_2, J(HPt) = 24], 4.45 and 3.05 (AB spin system, 8 H, $ArCH_2Ar$, ^2J = 13.4), 4.12 (s, 4 H, OCH_2CONEt_2), 3.37 (q, 4 H, NCH_2CH_3, ^3J = 7.0), 3.03 (q, 4 H, NCH_2CH_3, ^3J = 7.0), 1.30 (s, 18 H, Bu^t), 1.16 (t, 6 H, NCH_2CH_3, ^3J = 7.0), 1.12 (t, 6 H, NCH_2CH_3, ^3J = 7.0 Hz) and 0.78 (s, 18 H, Bu^t). ^{13}C-{^1H} NMR ($CDCl_3$): δ 166.52 (s, C=O), 152.26–124.81 (aromatics), 112.83 [m, $C(CN)_2$], 72.10 [d, OCH_2PPh_2, J(PC) = 38 Hz], 71.71 (s, OCH_2CONEt_2), 40.54 and 39.99 (s, NCH_2CH_3), 33.74 and 33.56 [2s, $C(CH_3)_3$], 31.39 and 30.88 [2s, $C(CH_3)_3$], 30.47 (2s, $ArCH_2Ar$), 14.08 and 12.83 (2s, NCH_2CH_3). ^{31}P-{^1H} NMR ($CDCl_3$): δ 11.93 [s with Pt satellites, PPh_2, J(PPt) = 3621 Hz] [Found: C, 64.10; H, 5.65; N, 5.30. Calc. for $C_{88}H_{100}N_6O_6P_2Pt{\cdot}0.75CH_2Cl_2$ (M_r = 1594.85 + 63.70): C, 64.25; H, 6.15; N, 5.05%].

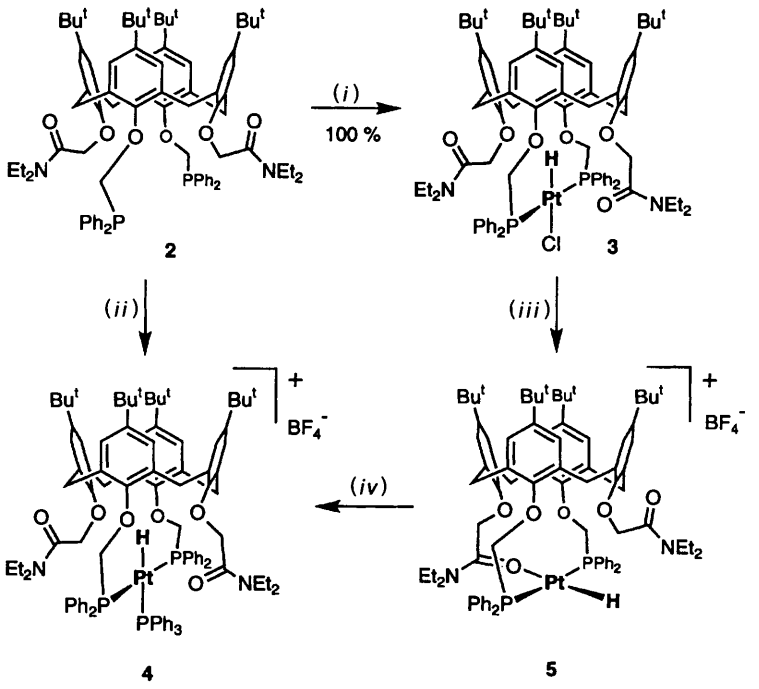

Scheme 1 (*i*) *trans*-[PtH(Cl)(PPh$_3$)$_2$], CH_2Cl_2; (*ii*) [PtH(thf)(PPh$_3$)$_2$]BF_4, CH_2Cl_2, tetrahydrofuran (thf); (*iii*) $AgBF_4$, CH_2Cl_2, thf; (*iv*) PPh_3, CH_2Cl_2

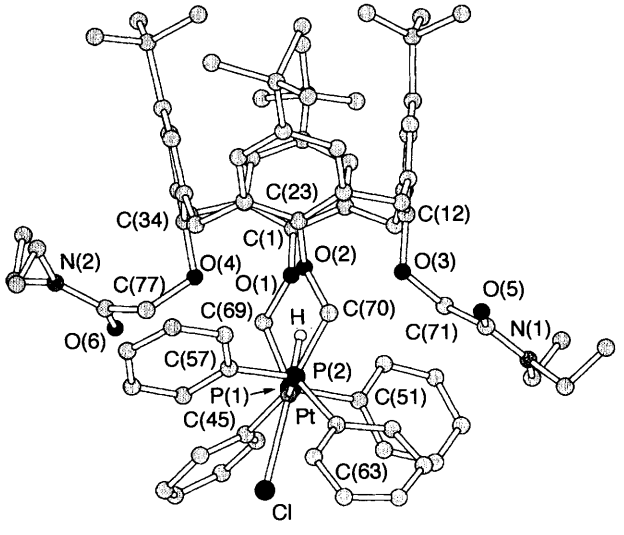

Fig. 1 MolView drawing of complex **3**. Hydrogen atoms, except for the hydride ligand, are omitted for clarity. Selected bond distances (Å) and angles (°): Pt–H 1.50(9), Pt–Cl 2.408(4), Pt–P(1) 2.256(5), H···O(1) 2.4(1), H···O(2) 2.7(1), O(1)···O(2) 4.14(3), O(3)···O(4) 5.05(3), Pt–P(2) 2.268(5); Cl–Pt–H 175(5), P(1)–Pt–P(2) 164.3(2), Pt–P(1)–C(69) 112.4(5), C(45)–P(1)–C(51) 102.8(8), Pt–P(2)–C(70) 112.4(6), C(57)–P(2)–C(63) 117.0(5), C(1)–O(1)–C(69) 114(1), C(23)–O(2)–C(70) 114(1). Dihedral angles between the facing aryl rings of the calixarene matrix: 80.1(4) and 14(1)°

intimate contact with methylene groups situated on each of the four pendant arms and also with the axial H atoms of the methylene units of the calixarene itself. The two amide groups are equivalent in NMR terms. These considerations lead to the postulated structure of **3** (shown in Scheme 1) having the hydride ligand inside the cavity defined by the pendant arms ('inside' form). The result of the crystal-structure analysis of **3** confirms the conclusion drawn from the NMR study (Fig. 1).*

The calixarene matrix persists in the cone conformation, with two of the facing phenolic rings being almost parallel and the other two being essentially perpendicular. The co-ordination geometry about the platinum atom deviates somewhat from idealized square planarity. In particular, the P–Pt–P angle [164.3(2)°] is such that the metal atom is pushed out of the cavity. Presumably, the short pendant arms cause steric strain at the metal centre, which must adopt a *trans* configuration, resulting in the slightly distorted geometry. The short arms also ensure that the bound platinum atom is in a rather close contact with oxygen atoms O(3) and O(4) on the spectator arms. These oxygen atoms prevent gyroscopic spinning[10] of the H–Pt–Cl group around the P–P axis [Pt–Cl 2.408(4), Pt–O(4) 3.67(4), Pt–O(3) 4.05(4) Å] so that extrusion of the H atom from the cavity is prohibited. This hypothesis is corroborated by our observation that the hydride NMR signal remains unchanged over a wide temperature range (−80 to +30 °C, 500 MHz), with no indication of interconversion of 'inside' and 'outside'

* Crystal data for **3** ($C_{82}H_{101}ClN_2O_6P_2Pt{\cdot}CH_2Cl_2{\cdot}C_6H_{14}$). M = 1674.33, colourless crystals, 0.25 × 0.25 × 0.30 mm, monoclinic, space group $C2/c$, a = 22.544(15), b = 14.244(4), c = 53.441(29) Å, β = 97.70(5)°, U = 17 006(15) Å^3, Z = 8, ρ_{calc} = 1.244 g cm^{-3}, $F(000)$ = 6976, μ = 18.48 cm^{-1}. A suitable crystal of **3** was obtained by slow diffusion of hexane into a dichloromethane solution of it at room temperature. Data were collected on an Enraf-Nonius CAD4 diffractometer at room temperature with graphite-monochromated Mo-Kα radiation (λ = 0.7107 Å). The cell parameters were obtained by fitting a set of 25 high θ reflections. The data collection [ω–2θ scan type, $2\theta_{max}$ = 46°, $+h+k\pm l$, intensity controls without appreciable decay (0.2%)] gave 12 732 reflections from which 4724 were independent (R_{int} = 0.025) with $I > 3\sigma(I)$. After Lorenz, polarization and absorption (DIFABS)[7] corrections, the structure was solved by direct methods, revealing many non-hydrogen atoms of the molecule. The remaining atoms were found after successive structure factor and Fourier-difference calculations. After isotropic (R = 0.073), then anisotropic refinement (R = 0.063), many hydrogen atoms could be found using a Fourier-difference map, in particular the Pt–*H* atom (*ca.* 0.44 e Å^{-3}). Some atoms of the main molecule were refined isotropically due to disorder and/or large thermal coefficients. The whole structure was refined by full-matrix least-squares techniques (on F); 757 variables and 4724 observations; $w = 1/\sigma(F_o)^2 = [\sigma^2(I) + (0.04F_o^2)^2]^{-\frac{1}{2}}$ with the resulting R = 0.055, R' = 0.061 and S = 3.622 (residual Δρ ≤ 0.37 e Å^{-3}). Atomic scattering factors were taken from ref. 8. All calculations were performed on a Digital Micro VAX 3100 computer with the MOLEN[9] package. Atomic coordinates, thermal parameters, and bond lengths and angles have been deposited at the Cambridge Crystallographic Data Centre (CCDC). See Instructions for Authors, *J. Chem. Soc., Dalton Trans.*, 1996, Issue 1. Any request to the CCDC for this material should quote the full literature citation and the reference number 186/275.

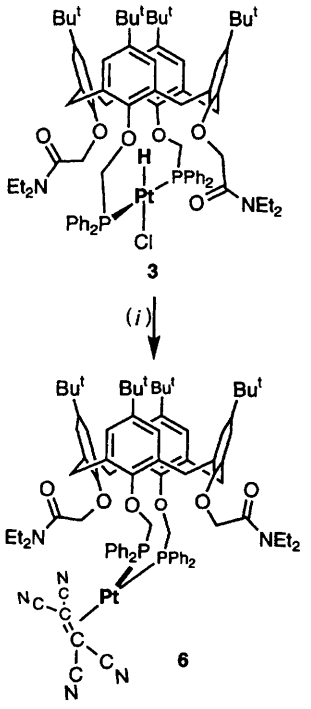

Scheme 2 (*i*) $(NC)_2C{=}C(CN)_2$, $CHCl_3$

forms. It is interesting to consider that hydrogen bonding between the intracavity hydride and phenolic oxygen atoms imposes an additional barrier to rotation of the H–Pt–Cl unit. Examination of the solid-state structure shows that two of the oxygen atoms [O(1) and O(2)] lie sufficiently close to the hydride so as to enter into weak hydrogen bonds [H • • • O(1) 2.4(1), H • • • O(2) 2.7(1) Å].

A remarkable feature of this reaction concerns the exceptionally high specificity for cyclisation which allows formation of **3** in essentially 100% yield. It is conceivable that formation of the 16-membered metallocycle is driven by a template effect of the adjacent amide groups. Thus, interaction between the oxygen-donor atoms and the emerging monophosphorus adduct will tend to centralise the platinum core such that intramolecular attachment to the second phosphine is highly favoured whilst inhibiting intermolecular association (*i.e.* polymer formation). Support for this notion is provided by separate studies in which it was found that less efficient cyclisation occurs when weaker donors replace the amide groups. Interestingly, hydride **4**, prepared by reacting **2** with $[PtH(thf)(PPh_3)_2]^+$, was also formed in high yield (Scheme 1).

It is important from the point of view of future applications to note that complex **3** undergoes substitution reactions at the exposed chlorine (Scheme 1). Indeed it was found that the chlorine atom was easily abstracted with $AgBF_4$ yielding the intermediary cationic complex **5** which provides access to a range of end-capped platinum hydrides, *e.g.* **4**, retaining the 'inside' form. Importantly the nature of the terminal (exposed) ligand can be controlled so as to modulate the electron properties of the Pt–H bond. Facile removal of the chlorine with subsequent formation of **5** is promoted by the co-ordinating ability of the amide function such that the co-ordination plane in **5** lies parallel to the lower rim of the calixarene. Incidentally, the regions immediately above and below the platinum centre in **5** are markedly disparate.

Availability of this family of organometallic calixarenes is expected to provide many important opportunities for selective homogeneous transformations. The structure of these complexes permits exploration of two generalized metal-centred reactions; namely reactions inside and outside the cavity. So far we have shown the accessibility of the organometallic fragment for promoting reaction outside the cavity. This is demonstrated clearly by the reaction between **3** and tetracyanoethylene (tcne) resulting in rapid and quantitative formation of the platinum(0) complex **6** (Scheme 2). The presence of co-ordinated tcne lying outside the cavity was shown by an X-ray diffraction study.

In conclusion, the 18-membered diphosphine **2** appears particularly well suited for the formation of encapsulated platinum hydrides. Systems such as **3** and **4** clearly open the way to transition-metal-controlled transformations occurring inside a molecular cavity.

Acknowledgements

We are grateful to Professor A. Harriman (Ecóle Européenne de Chimie, Polymères et Matériaux, ECPM) for useful discussion.

References

1 See, for example, C. D. Gutsche, *Monographs in Supramolecular Chemistry: Calixarenes*, ed. J. F. Stoddart, The Royal Society of Chemistry, Cambridge, 1989.
2 C. Wieser, C. B. Dieleman and D. Matt, *Coord. Chem. Rev.*, in the press; L. Giannini, E. Solari, A. Zanotti-Gerosa, C. Floriani, A. Chiesi-Villa and C. Rizzoli, *Angew. Chem., Int. Ed. Engl.*, 1996, **35**, 85.
3 J. C. J. Bailar and H. Itatani, *Inorg. Chem.*, 1965, **4**, 1618.
4 C. Loeber, C. Wieser, D. Matt, A. De Cian and J. Fischer, *Bull. Soc. Chim. Fr.*, 1995, **132**, 166.
5 C. Jaime, J. de Mendoza, P. Prados, P. M. Nieto and C. Sánchez, *J. Org. Chem.*, 1991, **56**, 3372.
6 P. S. Pregosin and R. W. Kunz, in *^{31}P and ^{13}C NMR of Transition Metal Phosphine Complexes*, eds. P. Diehl, E. Fluck and R. Kosfeld, Springer, Berlin-Heidelberg, 1979.
7 N. G. Walker and D. Stuart, DIFABS, *Acta Crystallogr., Sect. A*, 1983, **39**, 158.
8 *International Tables for X-Ray Crystallography*, D. Riedel, Boston, MA, 1983, A, 183.
9 C. K. Fair, MOLEN, An Interactive Intelligent System for Crystal Structure Analysis, Enraf-Nonius, Delft, 1990.
10 G. M. Gray and C. H. Duffey, *Organometallics*, 1994, **13**, 1542.

Received 19*th August* 1996; *Communication* 6/05764K